AIP | Journal of Applied Physics

Tunable strain effect and ferroelectric field effect on the electronic transport properties of La0.5Sr0.5CoO3 thin films

Q. X. Zhu, W. Wang, X. Q. Zhao, X. M. Li, Y. Wang et al.

Citation: J. Appl. Phys. **111**, 103702 (2012); doi: 10.1063/1.4716188
View online: http://dx.doi.org/10.1063/1.4716188
View Table of Contents: http://jap.aip.org/resource/1/JAPIAU/v111/i10
Published by the American Institute of Physics.

Tunable strain effect and ferroelectric field effect on the electronic transport properties of $La_{0.5}Sr_{0.5}CoO_3$ thin films

Q. X. Zhu,[1,2] W. Wang,[1] X. Q. Zhao,[1] X. M. Li,[1] Y. Wang,[3] H. S. Luo,[1] H. L. W. Chan,[3] and R. K. Zheng[1,3,a)]

[1]*State Key Laboratory of High Performance Ceramics and Superfine Microstructure, Shanghai Institute of Ceramics, Chinese Academy of Sciences, Shanghai 200050, China*
[2]*Graduate School of Chinese Academy of Sciences, Beijing 100039, China*
[3]*Department of Applied Physics and Materials Research Center, The Hong Kong Polytechnic University, Hong Kong, China*

(Received 21 December 2011; accepted 14 April 2012; published online 17 May 2012)

Tensiled $La_{0.5}Sr_{0.5}CoO_3$ (LSCO) thin films were epitaxially grown on piezoelectric 0.67Pb$(Mg_{1/3}Nb_{2/3})O_3$-0.33$PbTiO_3$ (PMN-PT) single-crystal substrates. Due to the epitaxial nature of the interface, the lattice strain induced by ferroelectric poling or the converse piezoelectric effect in the PMN-PT substrate is effectively transferred to the LSCO film and thus reduces the tensile strain of the film, giving rise to a decrease in the resistivity of the LSCO film. We discuss these strain effects within the framework of the spin state transition of Co^{3+} ions and modification of the electronic bandwidth that is relevant to the induced strain. By simultaneously measuring the strain and the resistivity, quantitative relationship between the resistivity and the strain was established for the LSCO film. Both theoretical calculation and experimental results demonstrate that the ferroelectric field effect at room temperature in the LSCO/PMN-PT field-effect transistor is minor and could be neglected. Nevertheless, with decreasing temperature, the ferroelectric field effect competes with the strain effect and plays a more and more important role in influencing the electronic transport properties of the LSCO film, which we interpreted as due to the localization of charge carriers at low temperature. © *2012 American Institute of Physics*. [http://dx.doi.org/10.1063/1.4716188]

I. INTRODUCTION

Seriously Sr-doped lanthanum cobalt oxide thin film, $La_{0.5}Sr_{0.5}CoO_3$ (LSCO), has received considerable attention due to their promising applications and a range of novel properties.[1–3] Transition-metal oxides containing Co^{3+} ions are of special interest among strongly-correlated systems because these oxides possess an extra degree of freedom in addition to the spin, charge, lattice, and orbital degrees of freedom. Namely, the possibility to change the spin state of Co^{3+} ions by modifying the delicate balance between the crystal-field splitting Δ_{CF} and the intra-atomic Hund exchange.[4] Since Δ_{CF} is very sensitive to the variation of Co-O bond length,[5] subtle structural changes can modify the spin state of Co^{3+} ions and thus, the physical properties of lanthanum cobalt oxides, e.g., resistivity,[6] magnetoresistance,[7,8] and electronic phase separation.[9] Large responses of electronic transport properties to substrate-induced lattice strain have been reported for $La_{1-x}Sr_xCoO_3$ thin films.[10–12] The commonly applied method for studying the lattice strain effect is the growth of thin films on single-crystal substrates with certain lattice mismatch, with the thickness of these thin films varying over a relatively large range. However, the properties of $La_{1-x}Sr_xCoO_3$ thin films are not only sensitive to lattice strain but also to oxygen content, crystalline quality, growth induced disorder, etc.[12–15] Particularly, it should be emphasized that the electronic transport properties of epitaxial $La_{1-x}Sr_xCoO_{3-\delta}$ thin films are highly sensitive to the oxygen nonstoichiometry δ, whose value strongly depends on the pressure at which the films were deposited or thermally post-treated.[13–15] Liu *et al.*[14] reported that the incorporation of oxygen vacancies seriously damages the conductivity of $La_{0.5}Sr_{0.5}CoO_{3-\delta}$ films and causes the expansion of the *c*-axis lattice constant of the films. Madhukar *et al.*[15] observed that $La_{0.5}Sr_{0.5}CoO_{3-\delta}$ films change from metallic to insulating behavior with increasing oxygen deficiencies. These results strongly indicate that, in addition to the lattice strain, oxygen content plays a very important role in determining the electronic transport and structural properties of LSCO films. To obtain a comprehensive and quantitative understanding of the intrinsic lattice strain effect of LSCO films, it is highly important that the studied LSCO films have exactly the same oxygen content.

Ferroelectric $(1-x)Pb(Mg_{1/3}Nb_{2/3})O_3$-$xPbTiO_3$ single crystals with composition near the morphotropic phase boundary ($x \sim 0.33$) display large remnant ferroelectric polarization, low coercive field, excellent piezoelectric activity[16] and have perovskite structure with lattice constants $a \sim b \sim c \sim 4.02$ Å.[17] Because of the good ferroelectric, piezoelectric, and structural properties of $(1\text{-}x)Pb(Mg_{1/3}Nb_{2/3})O_3$-$xPbTiO_3$ single crystals, they are very good materials for use as ferroelectrically and piezoelectrically active substrates. Perovskite $La_{1-x}A_xMnO_3$ (A = Ca, Sr, Ba)[18–21] and $La_{1-x}Sr_xCoO_3$ ($x = 0, 0.3$)[10,22] have been epitaxially grown on $(1-x)Pb(Mg_{1/3}Nb_{2/3})O_3 - xPbTiO_3$ ($x \sim 0.28, 0.33$) substrates, and it has been demonstrated that the lattice strain of these

a)Electronic mail: zrk@ustc.edu.

films can be reversibly modulated via the converse piezoelectric effect of the piezoelectric substrates. If LSCO films were epitaxially grown on the piezoelectric $0.67Pb(Mg_{1/3}Nb_{2/3})O_3$-$0.33PbTiO_3$ (PMN-PT) single crystals to form LSCO/PMN-PT structures, it is expected that the strain induced by ferroelectric poling or the converse piezoelectric effect in the PMN-PT would be *in situ* transferred to epitaxial LSCO films while keeping aforementioned extrinsic variables (e.g., oxygen content) fixed.

In this paper, we report our study on a heterostructure that consists of LSCO films epitaxially grown on PMN-PT single crystals. Due to the epitaxial nature of the interface, electric-field-induced strain in the PMN-PT crystal was effectively transferred to the LSCO film, which leads to a modulation of the resistivity of the LSCO film. Moreover, we have observed that the resistivity of the LSCO film is linearly dependent on the electric field applied to the poled PMN-PT substrate and established quantitative relationship between the resistivity and the induced strain for the LSCO film. These induced strain effects are believed to be closely related to the spin state of Co^{3+} ions and the effective electronic bandwidth linked to the electric-field-induced reduction in the in-plane tensile strain of the LSCO film. Furthermore, we have found that the ferroelectric field effect competes with the strain effect with decreasing temperature from room temperature and finally dominates over the strain effect for $T < 230$ K, obtaining new insight into the interface strain coupling effect and the ferroelectric field effect in $La_{1-x}Sr_xCoO_3$/PMN-PT structures.

II. EXPERIMENTAL SECTION

High-quality PMN-PT single crystals with a size of Φ50 mm × 80 mm were grown by a modified Bridgman technique as described previously.[23] The as-grown single crystals were cut into rectangular plates with a dimension of 10 mm × 3 mm × 0.45 mm and with the plate normal in the ⟨001⟩ crystal direction. Such cut crystals were polished to an average surface roughness of less than 1 nm so that they can be used as substrates. Measurements of the leakage current of the polished substrates using a keithley 6517 A electrometer show that the resistance of these substrates is $\sim 3 \times 10^9$ Ω at 296 K.

LSCO films were deposited on polished PMN-PT single-crystal substrates using dc magnetron sputtering. The deposition was conducted in an argon-oxygen flow with 50% Ar and 50% O_2 at a pressure of 5 Pa and a substrate temperature of 700 °C. During deposition, the substrate holder rotated slowly in order to reduce the thickness variation of the films. After deposition, the films were *in situ* cooled to room temperature and postannealed in 1 atm of flowing O_2 at 700 °C for 30 min using a rapid thermal processor furnace to reduce oxygen deficiencies and to increase the crystallinity of the films. The thickness of the LSCO films is measured to be ~50 nm using a JSM-6700F scanning electron microscope.

X-ray diffraction (XRD) patterns of the LSCO/PMN-PT structure were recorded using a Bruker D8 Discover x-ray diffractometer. Fig. 1(a) shows a schematic diagram for *in situ* measurements of the electric-field-induced strain in the LSCO film and the PMN-PT substrate using XRD. The strain was induced by applying dc electric fields to the PMN-PT substrate through the bottom gold electrode and the LSCO film. Here, the LSCO film serves as the top electrode since the resistance of the LSCO film at room temperature (~1049 Ω) is much smaller than that (3×10^9 Ω) of the PMN-PT substrate. After aligning the x-ray beam with the film plane, the electric field was adjusted from 0 to 10 kV/cm in a step of 1 kV/cm, while all other parameters were kept fixed. XRD θ-2θ scans were made at 296 K during the application of an electric field E to the PMN-PT substrate.

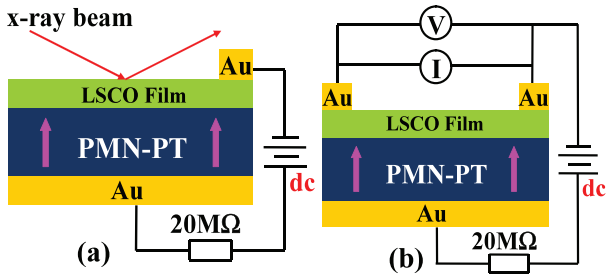

FIG. 1. Schematic diagrams of the LSCO/PMN-PT structure and the electric field configuration for *in situ* measurements of the strain (a) and the resistivity (b). The arrow in the PMN-PT represents the poling direction.

Figure 1(b) shows the resistivity measurement circuit for the LSCO/PMN-PT structure. A Keithley model 2400 source meter and a keithley model 2000 voltage meter were employed to measure the resistivity of the LSCO film between the two top-top gold electrodes in the temperature region from 32 to 296 K. The volume charge carrier density of the LSCO film was measured using a LakeShore Hall measurement system (LakeShore Cryotronics, Inc.). A laser interferometer (SIOS NT-04 Sensor) was employed to measure the electric-field-induced out-of-plane strain of the PMN-PT substrate as a function of bipolar electric voltage applied to the PMN-PT substrate at 296 K.

III. RESULTS AND DISCUSSION

Figure 2 shows the XRD θ-2θ scan of the LSCO/PMN-PT structure. Only (00l) (l = 1, 2, 3) diffraction peaks from the PMN-PT substrate and the LSCO film appear, indicating that the LSCO film is highly c-axis preferentially oriented. No diffraction peaks were detected that would be indicative of second phases. Note that the diffraction peak at $2\theta = 38.5°$ is the Au(111), originating from the top gold electrode. The out-of-plane lattice constant c of the LSCO film, calculated from the conventional θ-2θ scan data, is 3.8139 Å, which is smaller than that of the LSCO bulk (~3.853 Å[3]). The in-plane lattice constant a of the LSCO film was determined using the off-axis θ-2θ scan data [the inset (a) of Fig. 2] obtained by tilting the film plane at an angle of 45° and followed by the calculation using the equation $a = 2/\sqrt{(d_{101}^2 - d_{001}^2)}$, where d_{101} and d_{001} are the lattice spacings of the (101) and (001) planes, respectively.[24] The calculated in-plane lattice constant a is 3.9045 Å, which is larger than that of the LSCO bulk. In comparison with the lattice constants of the LSCO bulk, the decrease in the lattice

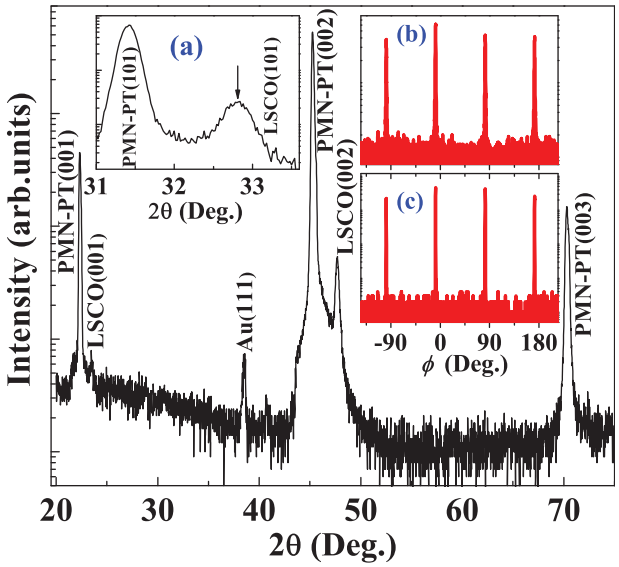

FIG. 2. X-ray diffraction pattern of the $La_{0.5}Sr_{0.5}CoO_3$/PMN-PT structure. The inset (a) is off-axis θ-2θ scan data obtained by tilting the film plane at an angle of 45°. The insets (b) and (c) show XRD phi scans on the $La_{0.5}Sr_{0.5}CoO_3$(101) and PMN-PT(101) diffraction peaks, respectively.

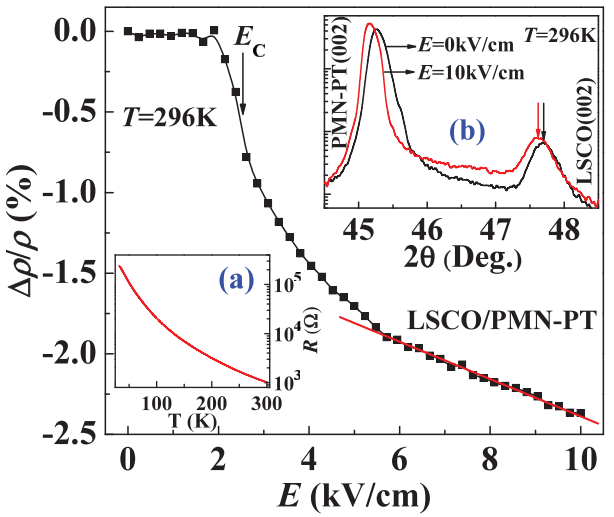

FIG. 3. Relative change in the resistivity of the $La_{0.5}Sr_{0.5}CoO_3$ film as a function of the electric field applied to the $La_{0.5}Sr_{0.5}CoO_3$/PMN-PT structure. The inset (a) shows temperature dependence of the resistance for the $La_{0.5}Sr_{0.5}CoO_3$ film when the PMN-PT substrate was in the P_r^0 state. The inset (b) shows the XRD patterns in the vicinity of (002) diffraction peaks for the $La_{0.5}Sr_{0.5}CoO_3$/PMN-PT structure under $E = 0$ and 10 kV/cm. The initial poling state of the PMN-PT substrate was in the P_r^0 state.

constant c and increase in the lattice constant a suggest that the LSCO film is subject to biaxial *tensile* strain ($c/a = 0.976$) in the plane of the film due to the large lattice mismatch between the LSCO film and the PMN-PT substrate. The in-plane epitaxial relationship between the LSCO film and the PMN-PT substrate was examined through XRD phi scans of the LSCO(101) and PMN-PT(101) planes. Two sets of fourfold symmetrical diffraction peaks originating from the LSCO film and the PMN-PT substrate [see the inset (b) and (c) of Fig. 2] were observed, indicating the epitaxial nature of the LSCO film on the PMN-PT substrate.

We measured the temperature dependence of the resistance for the LSCO film when the PMN-PT substrate was in the unpoled state and showed the results in the inset (a) of Fig. 3. Similar to the results found in $La_{0.7}Sr_{0.3}CoO_3$ thin films grown on $SrTiO_3$ (Ref. 10) and $0.72Pb(Mg_{1/3}Nb_{2/3})O_3$-$0.28PbTiO_3$ (Ref. 10) substrates with in-plane tensile strain, the resistance of the LSCO film increases with decreasing temperature from 300 K, which is in contrast to the metallic conductivity (i.e., $dR/dT > 0$) of the bulk LSCO single crystals.[6] The strain-induced static Jahn-Teller-type deformation of the CoO_6 units may provide a localization mechanism[10,25] for understanding the insulating behavior ($dR/dT < 0$) of the film. Besides, the insulating behavior could be resulted from the incorporation of oxygen vacancies which interrupt the Co-O-Co electron hopping networks, causing semiconducting behavior of the resistance.[14,26]

Figure 3 shows the relative change in the resistivity, $\Delta\rho/\rho$, of the LSCO film as a function of the electric field E applied to the LSCO/PMN-PT structure at a fixed temperature of 296 K. Here, $\Delta\rho/\rho$ is defined as $\Delta\rho/\rho = [\rho(E) - \rho(0)]/\rho(0)$ where $\rho(0)$ and $\rho(E)$ are the resistivity of the LSCO film under zero electric field and an electric field E, respectively. Initially, the PMN-PT substrate was in the unpoled state ($E = 0$ kV/cm, denoted by P_r^0) and E was increased from 0 to 10 kV/cm in a step of 0.24 kV/cm. The resistivity is virtually field-independent for $E \leq 2$ kV/cm but decreases considerably in the field region of 2 kV/cm $< E < 6$ kV/cm. For $E > 6$ kV/cm, the resistivity decreases linearly with increasing E, which is a typical behavior of the resistivity due to the converse piezoelectric effect of the PMN-PT substrate. The electric-field-induced decrease in the resistivity near the coercive field E_C of the PMN-PT substrate is similar to that observed in the $LaMnO_{3+\delta}$/PMN-PT structure where the lattice strain of the $LaMnO_{3+\delta}$ film was modified by the poling-induced strain in the PMN-PT substrate.[27] We have performed *in situ* XRD θ-2θ scan near the PMN-PT(002) and LSCO(002) diffraction peaks under the application of electric fields to the PMN-PT substrate and observed that the out-of-plane strain of both the PMN-PT substrate and the LSCO film were altered due to the electric-field-induced poling of the PMN-PT substrate. Selected XRD patterns in the vicinity of the PMN-PT(002) and LSCO(002) diffraction peaks under $E = 0$ and 10 kV/cm are shown in the inset (b) of Fig. 3. The PMN-PT(002) and LSCO(002) diffraction peaks clearly shift towards lower 2θ angle when an electric field of $E = 10$ kV/cm was applied to the LSCO/PMN-PT structure, implying that the lattice constants c of the PMN-PT substrate and the LSCO film for $E = 10$ kV/cm are larger than those for $E = 0$ kV/cm. The electric-field-induced out-of-plane strain $\Delta\varepsilon_{zz}$, $\Delta\varepsilon_{zz} = [c(E) - c(0)]/c(0)$, for the PMN-PT substrate and LSCO film are 0.21% and 0.17%, respectively. For $E \geq 6$ kV/cm, the resistivity is almost linearly dependent on the electric field, i.e., $\Delta\rho/\rho \propto E$, which could be caused by the linear decrease in the in-plane tensile strain of the film induced by the electric-field-induced strain via the converse piezoelectric effect in the PMN-PT substrate, similar to that of $La_{1-x}A_xMnO_3$ (A = Ca,Sr,Ba)/PMN-PT system.[19–21] The electric-field-induced change in the lattice strain of the LSCO film is expected to cause changes in the spin state of Co^{3+} ions and

the effective electronic bandwidth. When a positive electric field [i.e., the direction of the electric field points toward the LSCO film, as schematically shown in Figs. 1(a) and 1(b)] is applied to the unpoled PMN-PT substrate, the electric field induces an in-plane compressive strain in the PMN-PT substrate due to the rotation of the polarization direction of ferroelectric domains toward the electric-field direction. The induced compressive strain was transferred to the epitaxial LSCO film, causing a reduction in the in-plane tensile strain of the LSCO film and thus giving rise to a decrease in the in-plane Co-O bond length and an increase in the Co-O-Co bond angle.[28] Since the electronic bandwidth W can be estimated from the Co-O bond length d and the Co-O-Co bond angle θ by using $W \propto \sin(\theta/2)/d^{3.5}$,[29] the reduction in d and the increase in θ both enhance W, favoring the active hopping of charge carriers, thus, increasing the volume fraction of ferromagnetic metallic phase.[9,30] A continuous increase in the magnetization has been observed with the piezoelectric compression in the plane of $La_{0.7}Sr_{0.3}CoO_3$ films grown on (001)-oriented $0.72Pb(Mg_{1/3}Nb_{2/3})O_3$-$0.28PbTiO_3$ substrates at 300 K,[10] which implies spin-state transition of Co^{3+} ions induced by compressive strain, from low-spin (LS) ($t_{2g}^6 e_g^0$ with S = 0) to high-spin (HS) ($t_{2g}^4 e_g^2$ with S = 2) or, more likely, an energetically close intermediate spin (IS) ($t_{2g}^5 e_g^1$ with S = 1) states.[31,32] Accompanied with the spin state transition of Co^{3+} ions, the compressive stress increases the number of the mobile e_g electrons, thereby reducing the resistivity of the LSCO film.

Poled ferroelectric materials possess the converse piezoelectric effect; that is, applying an electric field E with the same polarity as the poling field to the poled ferroelectric materials will result in a linear expansion of the lattice of the materials along field direction. After the PMN-PT substrate had been poled, we studied the effects of the lattice strain induced by the converse piezoelectric effect on the lattice constants and transport properties of the LSCO film. In the inset (a) of Fig. 4, we show the relative change in the resistivity ($\Delta\rho/\rho$) of the LSCO film as a function of the electric field E applied to the poled PMN-PT substrate at $T = 296$ K. Note that the resistivity was measured using the electrical measurement circuit shown in Fig. 1(b). During the measurements, the top and bottom gold electrodes were held at low and high potentials, respectively, so that the direction of the electric field is the same as that of the polarization. We found that the relative change in the resistivity $\Delta\rho/\rho$ decreases linearly with increasing E. Similar linear dependence of $\Delta\rho/\rho$ on E has also been observed at low temperatures (32 K $\leq T <$ 296 K). The relationship between $\Delta\rho/\rho$ and E can be described by $\Delta\rho/\rho = aE$, where a is a negative constant. To obtain a quantitative relationship between the resistivity and the lattice strain for the LSCO film, we further examined the electric-field-induced lattice strain in the PMN-PT substrate and the LSCO film by measurements of the PMN-PT(002) and LSCO(002) diffraction peaks under electric fields at a fixed temperature of 296 K using XRD. As shown in Fig. 4, the electric-field-induced strain along the field-direction in the PMN-PT substrate (i.e., out-of-plane strain $\varepsilon_{zz(PMN-PT)}$) increases linearly with increasing E. The relationship between $\varepsilon_{zz(PMN-PT)}$ and E can be described by $\varepsilon_{zz(PMN-PT)} = bE$, where b is a positive constant. In fact, the

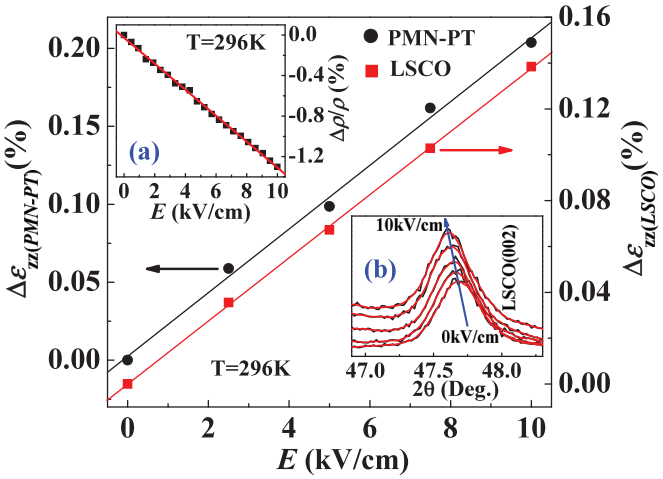

FIG. 4. Electric-field-induced out-of-plane strain for the PMN-PT substrate and the $La_{0.5}Sr_{0.5}CoO_3$ film as a function of the electric field applied to the $La_{0.5}Sr_{0.5}CoO_3$/PMN-PT structure at 296 K. The inset (a) shows the relative change in the resistivity, $\Delta\rho/\rho$, of the $La_{0.5}Sr_{0.5}CoO_3$ film as a function of the electric field. The inset (b) shows the XRD patterns in the vicinity of LSCO(002) diffraction peak under different electric fields. Note that the PMN-PT substrate has already been poled to P_r^+ state before all measurements.

electric-field-induced lattice strain along the direction of electric field due to the converse piezoelectric effect can be theoretically calculated using $\varepsilon_{zz(PMN-PT)} = d_{33}E$, where d_{33} is the piezoelectric coefficient. Using $d_{33} = 2000$ pC/N, we found that the calculated values (black solid line) of $\varepsilon_{zz(PMN-PT)}$ agree well with those of $\varepsilon_{zz(PMN-PT)}$ obtained from XRD measurements, which gives evidence that the electric-field-induced lattice strain is caused by the converse piezoelectric effect. The increase in the $\varepsilon_{zz(PMN-PT)}$ with E would be accompanied by the decrease in the in-plane strain in the PMN-PT substrate, which can be transferred to the LSCO film and thus causes a decrease in the in-plane lattice constants and an increase in the out-of-plane lattice constant of the LSCO film. The inset (b) of Fig. 4 shows that the LSCO(002) diffraction peak shifts to lower 2θ angles with increasing electric field from 0 to 10 kV/cm, which implies that the out-of-plane lattice constant of the LSCO film increases under electric field, consistent with the above analysis of the strain variation with E. Based on these XRD results, the electric-field-induced lattice strain $\varepsilon_{zz(LSCO)}$ along the field-direction for the LSCO film was estimated using the equation $\varepsilon_{zz(LSCO)} = [c_{LSCO}(E) - c_{LSCO}(0)]/c_{LSCO}(0)$ where $c_{LSCO}(E)$ and $c_{LSCO}(0)$ are the out-of-plane lattice constant of the LSCO film under an electric field E and zero electric field, respectively. We plotted $\varepsilon_{zz(LSCO)}$ as a function of E in Fig. 4. It can be seen that $\varepsilon_{zz(LSCO)}$ increases with increasing E and can be described by $\varepsilon_{zz(LSCO)} = cE$, where c is a positive constant. Combining $\varepsilon_{zz(PMN-PT)} = bE$ with $\varepsilon_{zz(LSCO)} = cE$, the relationship between $\varepsilon_{zz(LSCO)}$ and $\varepsilon_{zz(PMN-PT)}$ can be written as $\varepsilon_{zz(LSCO)} = m\varepsilon_{zz(LSCO)}$ where m is a constant. Clearly, the induced strain in the PMN-PT substrate is not fully transferred to the LSCO film, probably due to the lattice relaxation caused by the relatively large lattice mismatch between the LSCO film and the PMN-PT substrate. The efficiency of the strain transferring from the PMN-PT substrate

to the LSCO film is $m = 70\%$. Based on the equations $\Delta\rho/\rho = aE$ and $\varepsilon_{zz(LSCO)} = cE$, one may obtain the quantitative relationship between the resistivity and the induced out-of-plane strain and can be expressed as $\Delta\rho/\rho = \beta\varepsilon_{zz(LSCO)}$, where β is a constant, indicating that the relative change in the resistivity is proportional to the induced out-of-plane strain in the LSCO film.

Since the PMN-PT is a ferroelectric material, the LSCO/PMN-PT structure can be viewed as a ferroelectric field effect transistor where the PMN-PT and LSCO are the gate and conductive channel, respectively. When a gate voltage is applied to the PMN-PT substrate, the areal charge carrier density of the LSCO film would be modified. The electric-field induced change in the areal charge carrier density Δn is expressed as $\Delta n = \Delta P/e$[33] where ΔP is the remnant polarization of the PMN-PT substrate. Using the polarization $P = 33.8\ \mu C/cm^2$ at $E = 10$ kV/cm shown in Fig. 6, Δn due to the remnant polarization is $\sim 2.11 \times 10^{14}/cm^2$. On the other hand, measurements of the Hall effect for the LSCO/PMN-PT structure showed that the areal charge carrier density n of the LSCO film is $5 \times 10^{16}/cm^2$ at 296 K. The relative change in the areal carrier density $\Delta n/n$ is calculated to be $\sim 0.42\%$. Therefore, the ferroelectric field effect in the LSCO/PMN-PT system is negligibly small at room temperature. In a free electron model, one could obtain the relationship that $\Delta\rho/\rho = -\Delta n/n$ [34,35] Namely, if only the ferroelectric field effect is considered, the resistivity of the LSCO film should increase by 0.42% when a 450 V (or 10 kV/cm) gate voltage is applied to the PMN-PT substrate, because of the depletion of holes in the LSCO film.[36] As seen in Fig. 3, the actual sign of the change in the resistivity of the LSCO film is opposite to those expected from the field effect. It is thus believed that the electric-field induced change in the resistivity is mainly strain-induced at $T = 296$ K.

To further clarify whether the modulation of the resistivity of the LSCO film is due to the electric-field-induced strain effect or the ferroelectric field effect, we measured the resistivity of the LSCO film as a function of bipolar gate electric field applied to the PMN-PT substrate at various fixed temperatures. It is noted here that, if the ferroelectric field effect plays a dominant role in influencing the electronic transport properties of the LSCO film, the resistivity-electric field (ρ-E) hysteresis loop should show a rectangular shape with the resistivity change exhibiting opposite signs for opposite directions of applied electric field, as previously observed in the $La_{1-x}Ba_xMnO_3(x = 0.1,0.15)/PbZr_{0.2}Ti_{0.8}TiO_3$ (Ref. 35) and $La_{0.8}Ca_{0.2}MnO_3/Pb((Zr_{0.2}Ti_{0.8})O_3$ (Ref. 37) ferroelectric field effect transistors. In contrast, if the ferroelectric-poling-induced strain effect plays a dominant role in influencing the transport properties, the ρ-E hysteresis loop should show a butterflylike shape with the resistivity change exhibiting the same sign for opposite directions of applied electric field, as previously observed in the $La_{0.7}Sr_{0.3}CoO_3/0.72Pb(Mg_{1/3}Nb_{2/3})O_3$-$0.28PbTiO_3$ structure[10] and the $La_{0.7}Ca_{0.15}Sr_{0.15}MnO_3/0.67Pb(Mg_{1/3}Nb_{2/3})O_3$-$0.33PbTiO_3$ structure.[38] Fig. 5(a) shows that the ρ-E hysteresis loop has a symmetrical butterflylike shape at 296 K, which is the typical behavior of the resistivity change due to the strain induced by the rotation of the polarization direction in the PMN-PT substrate.[10,19,27,38] Similar to the butterflylike resistivity change shown in Fig. 5(a), the electric-field-induced out-of-plane strain also shows a butterflylike hysteresis loop for the PMN-PT substrate [see Fig. 6], which strongly demonstrates that the butterflylike modulation of the resistivity is strain induced. Therefore, we believe that

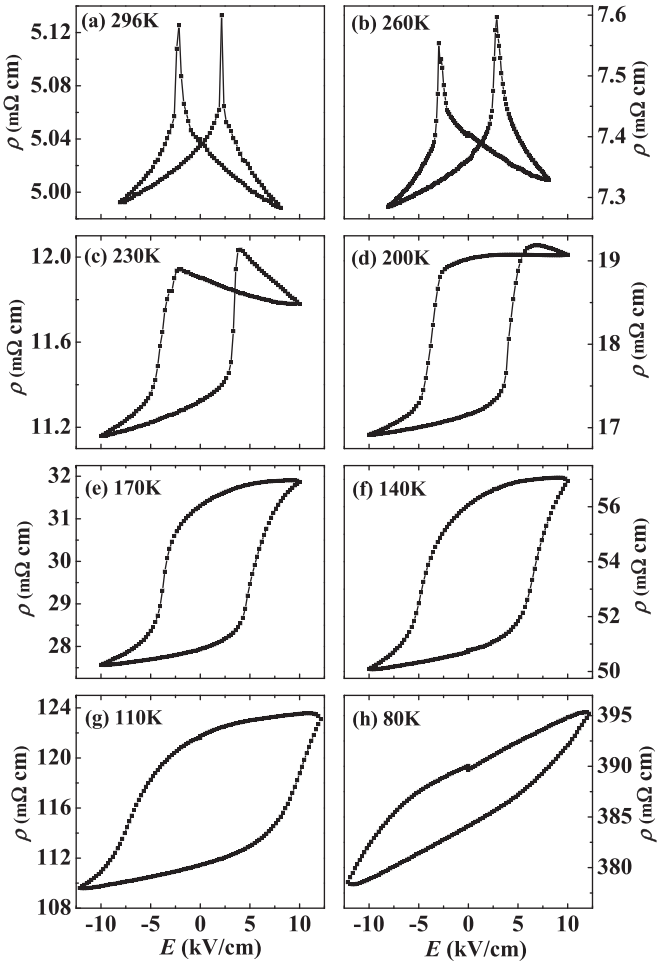

FIG. 5. Resistivity of the LSCO film at several fixed temperatures as a function of bipolar electric field applied to the PMN-PT substrate.

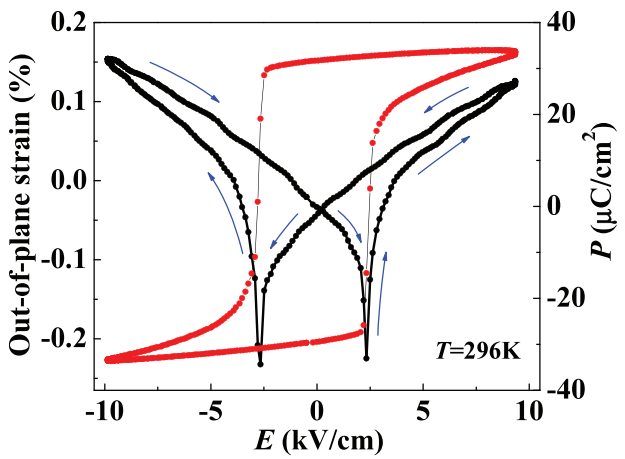

FIG. 6. Polarization-electric field hysteresis loop of the PMN-PT substrate measured at 296 K, and the electric-field-induced out-of-plane strain as a function of bipolar gate electric field applied to the PMN-PT substrate at 296 K.

the ferroelectric field effect has a minor effect on the electronic transport properties of the LSCO film at 296 K. Nevertheless, with decreasing temperature from 296 K, the symmetry of ρ-E hysteresis loop is reduced with the resistivity values for negative electric field lower than those for positive electric field [see Figs. 5(b) and 5(c)], which is ascribed to that the positive polarization of the PMN-PT layer will lead to a depletion of holes in the LSCO film and thus an increase in the resistivity, while the negative polarization of the PMN-PT layer will cause an accumulation of holes in the LSCO film and thus a decrease in the resistivity. The change of the ρ-E hysteresis loops from a butterflylike shape [Fig. 5(a)] to a rectangular-like shape [Figs. 5(d)–5(f)] indicates that the ferroelectric field effect plays a more and more important role in influencing the resistivity and finally dominates over the strain effect as the temperature decreases. At certain temperatures, e.g., $T = 230$ K, the ferroelectric field effect strongly competes with the strain effect, leading to the asymmetrical ρ-E shape [see Fig. 5(c)] which is undoubtedly due to the superposition of ferroelectric field effect and strain effect in the LSCO/PMN-PT structure. With further decreasing temperature, the rectangular-like ρ-E hysteresis loop starts shrinking and finally becomes extremely slim [see Fig. 5(h)]. Similar behaviors for the polarization-electric field (P-E) hysteresis loop have been observed in the 0.65Pb$(Mg_{1/3}Nb_{2/3})O_3$-0.35$PbTiO_3$ ceramics,[39] where a constant electric field of 12 kV/cm is apparently inadequate to align ferroelectric domains towards the field direction, leading to the gradual collapse of the P-E hysteresis loop. This feature is another evidence for that the ferroelectric field effect dominates over the strain effect at low temperatures. The enhanced ferroelectric field effect at low temperatures ($T \leq 230$ K) implies that the areal charge carrier density n in the LSCO film decreases with decreasing temperature, arising from the localization of the mobile charge carriers at low temperatures, which is directly reflected by the increase in the resistivity with decreasing temperature, as can be seen in the inset (a) of Fig. 3. The decrease in n corresponds to the increase in $\Delta n/n$, which can qualitatively explain the enhanced ferroelectric field effect with decreasing temperature.

IV. CONCLUSIONS

In summary, we examined the effects of substrate-induced strain on the lattice strain and electronic transport properties of LSCO film by *in situ* modifying the lattice strain of the LSCO film via ferroelectric poling or the converse piezoelectric effect of the PMN-PT substrate. We have found that the strain state and resistivity of the LSCO film can be modulated by the converse piezoelectric effect of the PMN-PT, and interpreted this behavior as due to the strain-induced spin state transition of Co^{3+} ions and modification of effective electronic bandwidth. Moreover, quantitative relationship between the resistivity and the induced strain has been established for the LSCO film, which could be important for understanding the physics of substrate-induced lattice strain effects for the $La_{1-x}Sr_xCoO_3$ systems. Surprisingly, it was found that the ferroelectric field effect competes with the strain effect with decreasing temperature from room temperature and finally dominates over the strain effect for $T < 230$ K, due to the localization of the charge carriers at low temperatures. The identification of the competing strain effect and ferroelectric field effect would be helpful for the theoretical modeling of the strain effect and the ferroelectric field effect in perovskite cobalt oxide film/PMN-PT systems.

ACKNOWLEDGMENTS

This work was supported by the National Science Foundation of China (Grant Nos. 51172259 and 11090332), the National Basic Research Program of China (973 Program, Grant No. 2009CB623304), the NSFC/RGC (Grant No. N_PolyU501/08), PolyU internal grant G-U846, and the Center for Smart Materials of the Hong Kong Polytechnic University.

[1]W. Jo, K. H. Kim, and T. W. Noh, Appl. Phys. Lett. **66**, 3120 (1995).
[2]B. Yang, S. Aggarwal, A. M. Dhote, T. K. Song, R. Ramesh, and J. S. Lee, Appl. Phys. Lett. **71**, 356 (1997).
[3]J. T. Cheung, P. E. D. Morgan, D. H. Lowndes, X. Y. Zheng, and J. Breen, Appl. Phys. Lett. **62**, 2045 (1993).
[4]P. M. Raccah and J. B. Goodenough, Phys. Rev. **155**, 932 (1967).
[5]M. A. Korotin, S. Y. Ezhov, I. V. Solovyev, V. I. Anisimov, D. I. Khomskii, and G. A. Sawatzky, Phys. Rev. B **54**, 5309 (1996).
[6]P. Ganguly, P. S. A. Kumar, P. N. Santhosh, and I. S. Mulla, J. Phys.: Condens. Matter **6**, 533 (1994).
[7]S. Yamaguchi, H. Taniguchi, H. Takagi, T. Arima, and Y. Tokura, J. Phys. Soc. Jpn. **64**, 1885 (1995).
[8]V. Golovanov, L. Mihaly, and A. R. Moodenbaugh, Phys. Rev. B **53**, 8207 (1996).
[9]D. N. H. Nam, K. Jonason, P. Nordblad, N. V. Khiem, and N. X. Phuc, Phys. Rev. B **59**, 4189 (1999).
[10]A. D. Rata, A. Herklotz, K. Nenkov, L. Schultz, and K. Dorr, Phys. Rev. Lett. **100**, 076401 (2008).
[11]M. Biasotti, L. Pellegrino, E. Bellingeri, N. Manca, A. S. Siri, and D. Marre, Appl. Phys. Lett. **97**, 223503 (2010).
[12]K. S. Hwang, H. M. Lee, S. S. Min, and B. A. Kang, J. Sol-Gel. Sci. Technol. **18**, 175 (2000).
[13]G. Prokhorov, G. G. Kaminsky, I. I. Kravchenko, and Y. P. Lee, Physica B **324**, 205 (2002).
[14]J. M. Liu and C. K. Ong, Appl. Phys. Lett. **73**, 1047 (1998).
[15]S. Madhukar, S. Aggarwal, A. M. Dhote, R. Ramesh, A. Krishnan, D. Keeble, and E. Poindexter, J. Appl. Phys. **81**, 3543 (1997).
[16]H. Cao, F. M. Bai, J. F. Li, D. Viehland, G. Y. Xu, H. Hiraka, and G. Shirane, J. Appl. Phys. **97**, 094104 (2005).
[17]B. Noheda, D. E. Cox, G. Shirane, J. Gao, and Z. G. Ye, Phys. Rev. B **66**, 054104 (2002).
[18]E.J. Guo, J. Gao, and H. B. Lu, Appl. Phys. Lett. **98**, 081903 (2011).
[19]R. K. Zheng, Y. Wang, J. Wang, K. S. Wong, H. L. W. Chan, C. L. Choy, and H. S. Luo, Phys. Rev. B **74**, 094427 (2006).
[20]C. Thiele, K. Dörr, O. Bilani, J. Rödel, and L. Schultz, Phys. Rev. B **74**, 054408 (2007).
[21]R. K. Zheng, Y. Jiang, Y. Wang, H. L. W. Chan, C. L. Choy, and H. S. Luo, Phys. Rev. B **79**, 174420 (2009).
[22]A. Herklotz, A. D. Rata, L. Schultz, and K. Dörr, Phys. Rev. B **79**, 092409 (2009).
[23]H. S. Luo, G. S. Xu, H. Q. Xu, P. C. Wang, and Z. W. Yin, Jpn. J. Appl. Phys. (Part 1) **39**, 5581 (2000).
[24]E. D. Specht, H. M. Christen, D. P. Norton, and L. A. Boatner, Phys. Rev. Lett. **80**, 4317 (1998).
[25]F. Fauth, E. Suard, V. Caignaert, B. Domenges, I. Mirebeau, and L. Keller, Eur. Phys. J. B **21**, 163 (2001).
[26]S. Aggarwal, A. M. Dhote, R. Ramesh, W. L. Warren, G. E. Pike, D. Dimos, M. V. Raymond, B. A. Tuttle, and J. T. Evans, Appl. Phys. Lett. **69**, 2540 (1996).

[27]R. K. Zheng, H. U. Habermeier, H. L. W. Chan, C. L. Choy, and H. S. Luo, Phys. Rev. B **81**, 104427 (2010).
[28]R. Lengsdorf, M. Ait-Tahar, S. S. Saxena, M. Ellerby, D. I. Khomskii, H. Micklitz, T. Lorenz, and M. M. Abd-Elmeguid, Phys. Rev. B **69**, 140403 (2004).
[29]P. G. Radaelli, G. Iannone, M. Marezio, H. Y. Hwang, S. W. Cheong, J. D. Jorgensen, and D. N. Argyriou, Phys. Rev. B **56**, 8265 (1997).
[30]R. Mahendiran and A. K. Raychaudhuri, Phys. Rev. B **54**, 16044 (1996).
[31]M. Imada, A. Fujimori, and Y. Tokura, Rev. Mod. Phys. **70**, 1039 (1998).
[32]V. G. Prokhorov, Y. P. Lee, K. W. Kim, V. M. Ishchuk, and I. N. Chukanova, Phys. Rev. B **66**, 132410 (2002).
[33]S. Gariglio, C. H. Ahn, D. Matthey, and J.-M. Triscone, Phys. Rev. Lett. **88**, 067002 (2002).
[34]C. H. Ahn, R. H. Hammond, T. H. Geballe, M. R. Beasley, J. M. Triscone, M. Decroux, O. Fischer, L. Antognazza, and K. Char, Appl. Phys. Lett. **70**, 206 (1997).
[35]T. Kanki, Y. G. Park, H. Tanaka, and T. Kawai, Appl. Phys. Lett. **83**, 4860 (2003).
[36]C. H. Ahn, A. Bhattacharya, M. Di Ventra, J. N. Eckstein, C. D. Frisbie, M. E. Gershenson, A. M. Goldman, I. H. Inoue, J. Mannhart, A. J. Millis, A. F. Morpurgo, D. Natelson, and J. M. Triscone, Rev. Mod. Phys. **78**, 1185 (2006).
[37]T. Zhao, S. B. Ogale, S. R. Shinde, R. Ramesh, R. Droopad, J. Yu, K. Eisenbeiser, and J. Misewich, Appl. Phys. Lett. **84**, 750 (2004).
[38]R. K. Zheng, H. U. Habermeier, H. L. W. Chan, C. L. Choy, and H. S. Luo, Phys. Rev. B **80**, 104433 (2009).
[39]S. P. Singh, A. K. Singh, D. Pandey, and S. Yusuf, Phys. Rev. B **76**, 054102 (2007).